

## Hippocampal Dentate Gyrus Atrophy Predicts Pattern Separation Impairment in Patients with LGI1 Encephalitis

Annika Hanert,<sup>a</sup> Julius Rave,<sup>a</sup> Oliver Granert,<sup>a</sup> Martin Ziegler,<sup>b†</sup> Anya Pedersen,<sup>c</sup> Jan Born,<sup>d</sup> Carsten Finke<sup>e</sup> and Thorsten Bartsch<sup>a\*</sup>

<sup>a</sup> Dept. of Neurology, Memory Disorders and Plasticity Group, University Hospital Schleswig-Holstein, University of Kiel, Arnold-Heller-Str. 3, 24105 Kiel, Germany

<sup>b</sup> Nanoelectronics, Technical Faculty, University of Kiel, Kaiserstr 2, 24143 Kiel, Germany

<sup>c</sup> Dept. of Psychology, Clinical Psychology and Psychotherapy, University of Kiel, Olshausenstr 62, 24118 Kiel, Germany

<sup>d</sup> Institute for Medical Psychology and Behavioral Neurobiology, University of Tübingen, Otfried-Müller-Str. 25, 72076 Tübingen, Germany

<sup>e</sup> Dept. of Neurology, Charité-Universitätsmedizin Berlin, Charitéplatz 1, 10117 Berlin, Germany

**Abstract**—Day-to-day life involves the perception of events that resemble one another. For the sufficient encoding and correct retrieval of similar information, the hippocampus provides two essential cognitive processes. Pattern separation refers to the differentiation of similar input information, whereas pattern completion reactivates memory representations based on noisy or degraded stimuli. It has been shown that pattern separation specifically relies on the hippocampal dentate gyrus (DG), whereas pattern completion is performed within CA3 networks. Lesions to these hippocampal networks emerging in the course of neurological disorders may thus affect both processes. In anti-leucine-rich, glioma-inactivated 1 (LGI1) encephalitis it has been shown in animal models and human imaging studies that hippocampal DG and CA3 are preferentially involved in the pathophysiology process. Thus, in order to elucidate the structure–function relationship and contribution of hippocampal subfields to pattern separation, we examined patients ( $n = 15$ , age range: 36–77 years) with the rare LGI1 encephalitis showing lesions to hippocampal subfields. Patients were tested 3.53 ± 0.65 years after the acute phase of the disease. Structural sequelae were determined by hippocampal subfield volumetry for the DG, CA1, and CA2/3. Patients showed an overall memory deficit including a significant reduction in pattern separation performance ( $p = 0.016$ ). In volumetry, we found a global hippocampal volume reduction. The deficits in pattern separation performance were best predicted by the DG ( $p = 0.029$ ), whereas CA1 was highly predictive of recognition memory deficits ( $p < 0.001$ ). These results corroborate the framework of a regional specialization of hippocampal functions involved in cognitive processing. © 2019 IBRO. Published by Elsevier Ltd. All rights reserved.

**Key words:** episodic memory, hippocampus-dependent memory, hippocampal sclerosis, hippocampal subfield segmentation, limbic encephalitis.

\*Corresponding author: Fax: +49-(0)431-500-23804.

E-mail addresses: [a.hanert@neurologie.uni-kiel.de](mailto:a.hanert@neurologie.uni-kiel.de) (A. Hanert), [julius-rave@gmx.de](mailto:julius-rave@gmx.de) (J. Rave), [o.granert@neurologie.uni-kiel.de](mailto:o.granert@neurologie.uni-kiel.de) (O. Granert), [martin.ziegler@tu-ilmenau.de](mailto:martin.ziegler@tu-ilmenau.de) (M. Ziegler), [pedersen@psychologie.uni-kiel.de](mailto:pedersen@psychologie.uni-kiel.de) (A. Pedersen), [Jan.Born@uni-tuebingen.de](mailto:Jan.Born@uni-tuebingen.de) (J. Born), [carsten.finke@charite.de](mailto:carsten.finke@charite.de) (C. Finke), [t.bartsch@neurologie.uni-kiel.de](mailto:t.bartsch@neurologie.uni-kiel.de) (T. Bartsch).

† Present address: Institute of Micro- and Nanoelectronics, Micro and Nanoelectronic Systems, Technical University Ilmenau, Gustav-Kirchhoff-Str. 1, 98693 Ilmenau, Germany.

**Abbreviations:** ANOVA, Analysis of Variance; CA, cornu ammonis; DG, dentate gyrus; eTIV, estimated total intracranial volume; FLAIR, fluid-attenuated inversion recovery; GC-DG, granule cell layer of the dentate gyrus; ISI, inter stimulus interval; LGI1, anti-leucine-rich, glioma-inactivated 1; MPRAGE, magnetization-prepared rapid gradient-echo; MRI, magnetic resonance imaging; mRS, modified Rankin scale; MST, Mnemonic Similarity Task; MWT-B, Mehrfachwahl-Wortschatz-Intelligenztest-B; PatSep score, Pattern Separation score; RAVLT, Rey auditory verbal learning test; RM score, Recognition Memory score; ROCF, Rey–Osterrieth complex figure; RWT, Regensburg word fluency test; TMT, Trail-Making Test.

## INTRODUCTION

In everyday life, we are experiencing a constant string of episodes that can be more or less similar with regard to time, objects, location and content. The formation of episodic memory, however, requires that similar experiences are transformed into unique and non-overlapping episodes that can be differentiated into distinct memories. To prevent these memories from interference and to ensure correct retrieval of newly encoded episodes, the hippocampus provides two neural operations which differentiate similar episodes and store them as distinct neural representations (McClelland et al., 1995; Knierim and Neunuebel, 2016; Rolls, 2016). First, a pattern separation process is critical for the separation and storage of similar and overlapping memory representations. During encoding, the neural

input is orthogonalized and de-correlated by associating distinct neural codes to the similar representations (Treves and Rolls, 1994). Secondly, pattern completion involves the reactivation of previously stored memories in case of noisy, incomplete or degraded input (Yassa and Stark, 2011). At retrieval, the pre-existing memory representation is reactivated as the overlapping input is used as a retrieval cue (McClelland et al., 1995; Norman and O'Reilly, 2003; Rolls, 2016). Animal models and human imaging studies suggest that the hippocampal dentate gyrus (DG) is particularly involved in pattern separation whereas CA3 is capable of performing both, pattern separation and completion computations depending on the variance of the sensory input (Lee et al., 2004; Leutgeb et al., 2004, 2007; Bakker et al., 2008; Berron et al., 2016). Animal findings show that neuronal ensembles in CA1 are also involved in pattern separation but differ from CA3 as they show a more linear input–output function in response to environmental changes. However, studies in humans characterizing the contribution of CA1 to pattern separation and completion are still scarce (Vazdarjanova and Guzowski, 2004).

In this context, the study of specific lesion models allows further clarification of the causal relationship of individual hippocampal subfield function and their operation in hippocampus-dependent memory processing (Bartsch et al., 2010, 2011; Döhring et al., 2017). Considering this, we examined patients with an anti-leucine-rich, glioma-inactivated 1 (LGI1) encephalitis who show lesion-associated and degenerative changes in hippocampal subfields. Patients who are positive for LGI1 antibodies develop limbic encephalitis and exhibit memory impairments and hippocampus-associated epileptic seizures in the acute stage (Irani et al., 2011, 2013; Malter et al., 2014), whereas in post-acute stages, significant and disabling memory deficits persist (Bettcher et al., 2014; Butler et al., 2014). Interestingly, the LGI1 gene transcript in the mouse is mainly expressed in the pyramidal and granular layers of the DG and CA3 field of the hippocampus, where the perforant path fibers from the entorhinal cortex project onto dendrites of the DG granule cells (Kalachikov et al., 2002; Herranz-Pérez et al., 2010; Bartsch and Wulff, 2015). Thus, the features of the LGI1 pathogenesis involving both the hippocampal DG and CA3 regions offer a lesion model to study the function of DG and CA3 within memory processing in the hippocampal network. In these patients, significant atrophy in the hippocampal CA2/3 and CA4/DG regions and a chronic memory impairment has been reported in the post-acute stage (Finke et al., 2017). Also, Miller et al. (2017) found a bilateral CA3 atrophy in patients with this rare form of limbic encephalitis.

The aim of the present study was to further elucidate the structure–function relationship and the contribution of hippocampal subfields to pattern separation in humans. We expected to find deficits in pattern separation in patients with LGI1 encephalitis as a result of hippocampal atrophy and as a consequence of limbic encephalitis (Malter et al., 2014). Against this background, inflammatory lesions particularly expressed in DG and CA3 that are characteristic of LGI1-antibody

mediated encephalitis should correlate with impairments in subfield-specific computations as seen in a greater variability in hippocampal subfield volumetry (Finke et al., 2017; Miller et al., 2017). Therefore, we tested LGI1 patients on a behavioral task, i.e., the Mnemonic Similarity Task (MST), that has been shown to tax hippocampal pattern separation (Kirwan and Stark, 2007; Stark et al., 2013; Hanert et al., 2017) and correlated task performance to structural sequelae in the hippocampus using high-resolution volumetry of the hippocampus. Hippocampal volumetry for the subfields of interest was assessed using the automated segmentation method Freesurfer 6.0.0.

## EXPERIMENTAL PROCEDURES

### Study cohort

Fifteen patients (mean age:  $64.47 \pm 3.28$  years, range: 36–77, 9 male) with anti-LGI1 encephalitis participated in the study. All reported data were collected after the acute stage of the limbic encephalitis with a mean time between symptoms onset and study examination of  $3.53 \pm 0.65$  years. Early symptoms of the limbic encephalitis before the onset of the acute phase (i.e., hippocampus-associated temporal lobe seizures, uni- or bilateral faciobrachial dystonic and other types of seizures) were reported by 10 patients (66%). The acute phase of limbic encephalitis was accompanied by typical clinical features such as amnesia, confusion, and behavioral and mood disturbances. Patients were moderately neurologically impaired measured by the modified Rankin Scale (mRS) score (mean:  $1.53 \pm 0.26$ , range: 0–3). Fifteen control participants (mean age:  $65.13 \pm 3.11$ , range: 40–80, 9 male) were individually matched according to sex, age and educational background including profession and years of formal education. The study was approved by the local ethics committee. All participants gave written informed consent for the procedures. The clinical and laboratory characteristics of some of these patients have been published (Finke et al., 2017). The present study provides an additional and new assessment of cognitive performance as well as a new analysis of the MRI data. The behavioral testing including neuropsychological assessment and acquisition of MRI data were no longer than 6 months apart.

### Behavioral tests

*Mnemonic similarity task.* Behavioral pattern separation was assessed by means of the Mnemonic Similarity Task (MST) (Kirwan and Stark, 2007; Stark et al., 2013) (<http://faculty.sites.uci.edu/starklab/mnemonic-similarity-task-mst/>). The computer-based task presents items on the screen as color photographs of everyday objects on a white background. The encoding phase included 128 items that had to be identified as either indoor or outdoor object. The immediate test phase comprised 192 items displaying in each case one third as exact repetitions of the encoded items (64 targets), similar

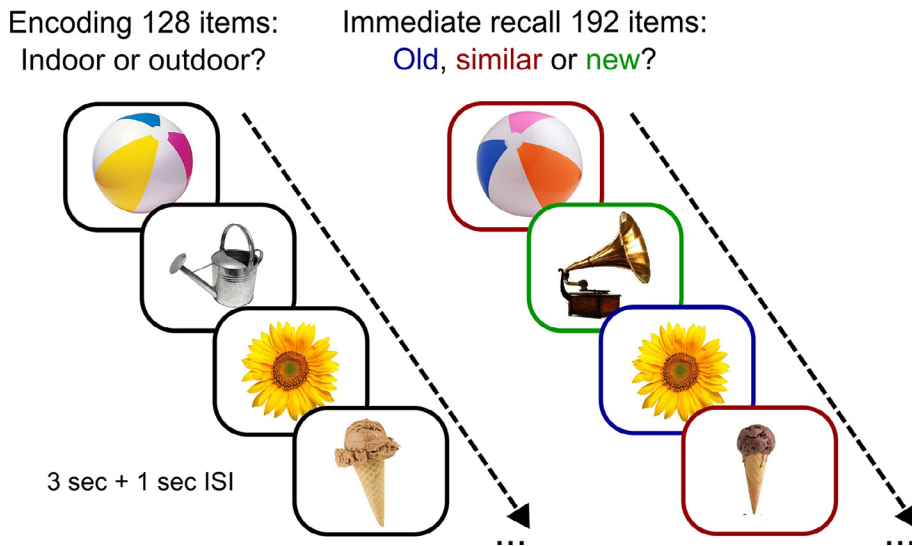


**Fig. 1.** Procedure of the MST. First, participants encoded 128 items of everyday objects by judging the items as indoor or outdoor objects. Then participants were supposed to decide whether the items were old, similar or new to the previously seen targets in an immediate recall condition containing 192 items. Displayed pictures are taken from the original image data base of the MST. ISI, inter-stimulus interval.

items (64 lures), and items that were totally new (64 foils). In this phase, participants indicated whether the objects were 'old', 'similar' or 'new' to the previously encoded targets. Of particular importance were the responses to lure items with the correct 'similar' response indicating successful pattern separation, whereas incorrect 'old' responses to lures suggest a bias toward pattern completion (Bakker et al., 2008; Yassa et al., 2010; Lacy et al., 2011). The lure objects were divided into five degrees of similarity to a target object ranging from 1 (most similar) to 5 (least similar). Therewith, behavioral pattern separation was also assessed as a function of lure similarity (Yassa et al., 2010; Lacy et al., 2011). In both the encoding and recall phases the stimuli were presented for 3 s with 1-s inter stimulus interval. For recording of data, participants had to respond via button press within the 3-s stimulus presentation (Fig. 1). By means of participants' responses at recall a Pattern Separation score (PatSep score) and a Recognition Memory (RM) score were computed each corrected for a response bias: i) *Pattern Separation (PatSep) score*:  $PatSep = [p \text{ (correct similar response to lures)} - p \text{ (false similar response to foils)}]$ , ii) *Recognition Memory (RM) score*:  $RM = [p \text{ (correct old response to targets)} - \text{(false old response to foils)}]$  (Yassa et al., 2010, 2011a; Stark et al., 2013).

**Neuropsychological assessment.** A comprehensive neuropsychological test battery was used to test episodic memory (Rey auditory verbal learning test, RAVLT) (Rey, 1941), visuospatial memory (Rey–Osterrieth complex figure, ROCF), working memory (digit span forwards and backwards), executive functioning (Trail-making Test A and B, TMT) (Reitan, 1979), verbal fluency (Regensburg word fluency test, RWT) (Aschenbrenner et al., 2000), and premorbid general intelligence (Mehr fachwahl–Wortschatz–Intelligenztest-B, MWT-B, as a

German equivalent of the National Adult Reading Test) (Lehrl, 2005) as described in Finke et al. (2017).

### MRI acquisition and hippocampal subfield segmentation

Whole-brain MRI were acquired using 3 Tesla MRI Scanners (Siemens Tim Trio, Siemens, Erlangen, Germany; Philips Achieva, Philips, Best, The Netherlands). T1-weighted MRI scans were recorded using a three-dimensional magnetization prepared rapid gradient-echo sequence (3D MPRAGE, matrix size =  $240 \times 240$ , 176 slices, voxel size =  $1 \times 1 \times 1 \text{ mm}^3$ ). The evaluation of clinical images was based on T2-weighted turbo spin echo sequences as well as a 3D isotropic T2-weighted fluid-attenuated inversion recovery (FLAIR).

Hippocampal subfield volumetric segmentation was performed on the T1-weighted scans using the freely available software Freesurfer image analysis suite version 6.0.0 (<http://surfer.nmr.mgh.harvard.edu/>). The standard processing steps of Freesurfer 6.0.0 are described as follows: first, non-brain tissues were removed using a hybrid watershed/surface deformation procedure (Ségonne et al., 2004). Then, images were automatically transformed to Talairach coordinates and subcortical white matter and deep gray matter volumetric structures containing the hippocampal formation were segmented (Fischl et al., 2004). The process was followed by intensity normalization (Sled et al., 1998) and tessellation of the gray matter/white matter boundary (Ségonne et al., 2007). The automated hippocampal subfield segmentation was performed by means of Bayesian inference and a probabilistic atlas of the hippocampal formation (Fischl et al., 2004; Van Leemput et al., 2009). The segmentation results were visually rechecked for accuracy in all subjects. Freesurfer 6.0.0. provides results regarding the volume of the alveus, parasubiculum, presubiculum, subiculum, CA1, CA2/3, CA4, granule cell layer of the DG (GC-DG), hippocampus–amygdala transition area, fimbria, molecular layer for subiculum and CA fields, hippocampal fissure and hippocampal tail. However, the analysis regarding hippocampal volumetry was hypothesis-driven and focused on the hippocampal regions of interest that are critically involved in pattern separation and completion processes (i.e. CA1, CA3 and DG) (Yassa and Stark, 2011). Given the segmented subfields by Freesurfer 6.0.0, the analyses thus included CA1, CA2/3, GC-DG, and CA4. The DG is originally formed by the granule cell, polymorphic, and molecular layers (Amaral et al., 2007). Freesurfer 6.0.0 assigns the DG's polymorphic and molecular layer to the CA4 region and keeps the DG separate with the layer of the

granule cells (Iglesias et al., 2015). Thus, we included CA4 to the GC-DG region in our analysis to make plausible predictions about the global DG and its contribution to hippocampal pattern separation. Throughout the analysis, we use the term “DG” referring to the volume of the segmented GC-DG and CA4 regions.

The updated technique of the Freesurfer 6.0.0 version provides significant advantages over the earlier method used in Freesurfer 5.3 described in (Van Leemput et al., 2009). Due to the use of an atlas based on ex vivo MRI data, the precision of the segmentation of subfield boundaries was improved that also affected the accuracy of hippocampal subfield volumes. Particularly, the delineation and segmentation of volumes of CA1 and CA2/3 are much more congruent with previous histological studies (Iglesias et al., 2015). The volumes of each subfield were corrected for inter-individual head size by means of the estimated total intracranial volume (eTIV). The correction was computed according to an atlas normalization formula (Buckner et al., 2004).

### Statistical analyses

The Shapiro–Wilk test was used for pretesting of normal distributions and Levene’s test was performed for the assessment of homogeneity of variances. Differences between the patient and control group were examined with paired samples *t*-tests or Wilcoxon signed–rank tests depending on distribution. Accordingly, confidence intervals were calculated for either the difference of the means or medians.  $2 \times 5$  repeated measures ANOVA with group as repeated factor (patient vs. control) and similarity (1 to 5) as within-subjects factor were performed to show differences in PatSep scores regarding lure similarities. Spearman’s  $\rho$  expressing the relation between PatSep scores and lure similarity was calculated for every participant separately and the mean correlation for both groups was calculated. Significances of the average correlations were tested using Wilcoxon signed–rank tests against zero. Depending on distribution Pearson’s *r* or Spearman’s  $\rho$  was used to characterize the relationship between the PatSep score and the RM score as well as the scores from the neuropsychological test battery. To analyze differences in hippocampal volume a three-way repeated measures ANOVA with group as repeated factor (patient vs. control) and subfield (CA1, CA2/3, DG) as well as side (left vs. right) as within-subject factors was conducted. Degrees of freedom were corrected according to Greenhouse–Geisser adjustment if the assumption of sphericity was violated. ANOVA were followed by planned post-hoc pairwise comparisons to specify significant main and interaction effects. To predict behavioral outcome variables (i.e., PatSep and RM scores) by hippocampal subfield volumes, multiple linear regression analyses were performed. The independence of residuals was checked by the Durbin–Watson statistic. For testing the distribution of residuals regarding normality, the Shapiro–Wilk test was performed. Homoscedasticity of residuals was tested using the Breusch–Pagan test. As the independent variables were correlated, the

established method of backward elimination was used to find best predictors of PatSep and RM scores. Adjustment for multiple testing was done using Benjamini & Hochberg’s False Discovery Rate. The significance level was set to  $p < 0.05$ , two-tailed for all tests. Data are specified as mean  $\pm$  SEM if not otherwise stated.

## RESULTS

### Mnemonic similarity task

Paired samples *t*-tests showed that pattern separation performance of LGI1 patients was significantly lower ( $22.01 \pm 4.60$ ) than the performance of controls ( $35.83 \pm 3.92$ ) ( $t(14) = 3.10$ ,  $p = 0.016$ , 95% CI [4.24, 23.41]). With regard to recognition memory, patients performed worse than controls (patients:  $65.67 \pm 6.02$ , controls:  $79.80 \pm 2.46$ ,  $t(14) = 2.56$ ,  $p = 0.023$ , 95% CI [2.31, 25.96]) (Fig. 2A). There was no significant correlation between pattern separation performance and recognition memory neither in the patient ( $r = 0.354$ ,  $p = 0.196$ ) nor in the control group ( $r = 0.420$ ,  $p = 0.120$ ). To further ensure that the pattern separation deficit was not secondary to a general impairment in recognition memory as well as to prevent that the results are biased by floor effects, we reran paired samples *t*-tests with the exclusion of patients ( $n = 3$ ) whose recognition performance was below 3 standard deviations from the mean of the control group ( $79.80 \pm 9.52$ ). The exclusion of highly impaired patients showed that recognition memory performance was equal in both groups (patients:  $75.00 \pm 3.65$ , controls:  $82.00 \pm 2.45$ ,  $t(11) = 1.78$ ,  $p = 0.102$ , 95% CI [−1.65, 15.65]), whereas pattern separation performance still differed significantly (patients:  $22.93 \pm 5.57$ , controls:  $34.38 \pm 4.73$ ,  $t(11) = 2.21$ ,  $p < 0.05$ , 95% CI [0.02, 22.88], no alpha adjustment).

Separate comparisons regarding the response types revealed no difference between the groups regarding the ‘old’ response to lures (patients:  $43.93 \pm 5.21$ , controls:  $42.93 \pm 2.82$ ,  $t(14) = -0.21$ ,  $p = 0.833$ , 95% CI [−11.01, 9.01]). In contrast, patients were more prone to incorrectly respond ‘new’ to lures (patients:  $26.87 \pm 5.35$ , controls:  $12.40 \pm 2.06$ ,  $t(14) = -2.90$ ,  $p = 0.017$ , 95% CI [−25.15, −3.78]). However, excluding the highly memory-impaired patients ( $\leq$  Q1 in recognition memory) led to equal results across groups regarding ‘new’ responses to lures (patients:  $19.25 \pm 4.12$ , controls:  $12.17 \pm 2.49$ ,  $t(11) = -1.98$ ,  $p = 0.074$ , 95% CI [−14.97, 0.80]). Results for paired samples *t*-tests for all response types are displayed in Fig. 2 B–D.

Entering the PatSep scores for 5 degrees of lure similarity in a  $2 \times 5$  repeated measures ANOVA revealed no group  $\times$  similarity interaction ( $F(4, 56) = 0.647$ ,  $p = 0.632$ ) but significant main effects for group ( $F(1, 14) = 10.03$ ,  $p = 0.007$ ) as well as similarity ( $F(4, 56) = 8.65$ ,  $p < 0.0001$ ). Post-hoc pairwise tests of simple effects demonstrated superior performance for the control group in every lure similarity, though not statistically significant for every degree (Lure 1:  $t(14)$

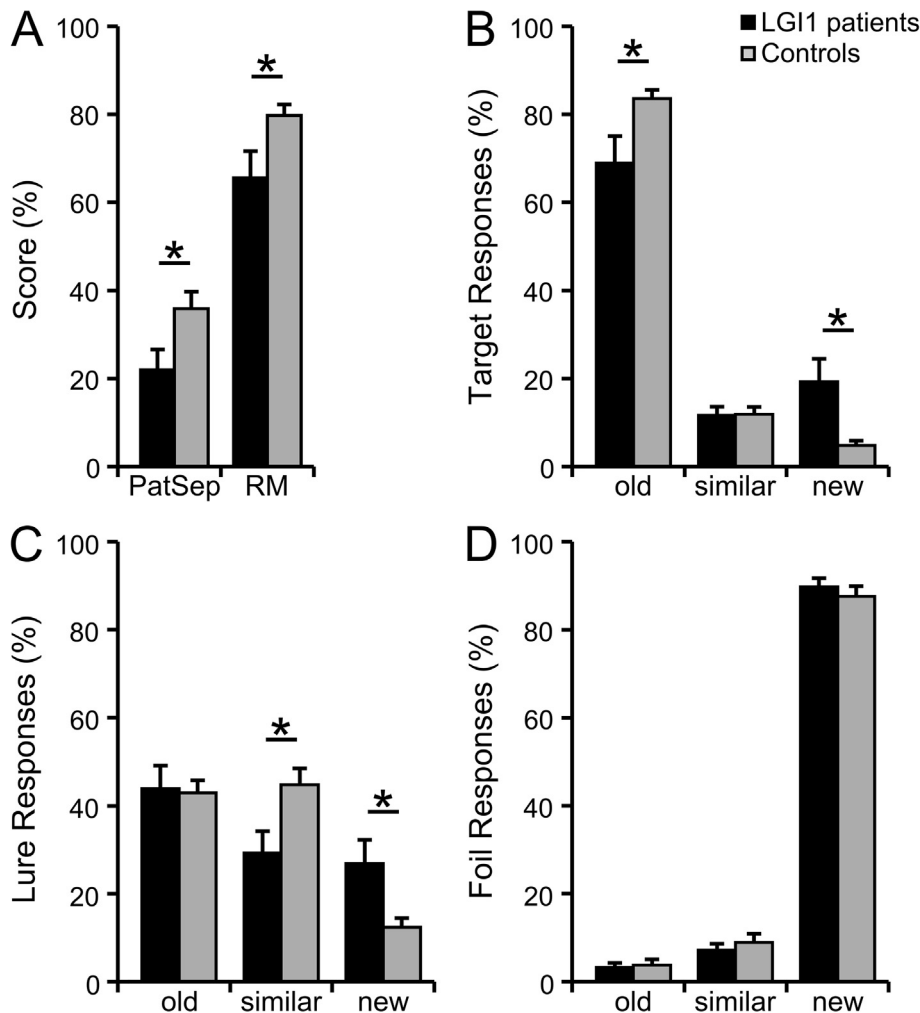


**Fig. 2.** Results of the MST including the PatSep and RM scores as well as all response types. Note that the PatSep and RM scores are bias corrected scores. Values of the response types are given in percent corresponding to the item types. Adjustment for multiple testing was done using Benjamini & Hochberg's False Discovery Rate.  $p < 0.05$ .

= 1.83,  $p = 0.088$ , 95% CI [-1.86, 23.81], Lure 2:  $t(14) = 3.17$ ,  $p = 0.034$ , 95% CI [5.39, 27.94], Lure 3:  $t(14) = 1.85$ ,  $p = 0.088$ , 95% CI [-1.53, 20.49], Lure 4:  $t(14) = 2.46$ ,  $p = 0.046$ , 95% CI [2.08, 30.22], Lure 5:  $t(14) = 2.66$ ,  $p = 0.046$ , 95% CI [3.21, 30.12]) (Fig. 3).

We further analyzed different degrees of lure similarity by means of a calculation of Spearman's rank correlation coefficients between lure similarity and the PatSep scores for every patient and control. The PatSep score was positively correlated with lure similarity for both the patient ( $r_s = 0.515 \pm 0.14$ ,  $Z = 2.84$ ,  $p = 0.008$ , for test against 0) and control group ( $r_s = 0.378 \pm 0.13$ ,  $Z = 2.36$ ,  $p = 0.018$ , for test against 0).

The results indicate that LGI1 patients were impaired in correctly separating lures from related targets. Notably, the same held true not only for the overall PatSep score but also for the scores related to lure similarities. The significant slope in pattern separation performance in both groups demonstrates that patients did not show a differential impairment in separating either highly similar or least similar lures as the deficit in

pattern separation was equally dispersed across all degrees of similarity (Fig. 3).

### Neuropsychological data

Patients were profoundly impaired in episodic verbal memory performance measured by the RAVLT (cf. Finke et al., 2017). They memorized fewer words throughout the five learning trials (patients:  $36.20 \pm 4.46$ , controls:  $60.67 \pm 1.97$ ,  $t(14) = 5.91$ ,  $p = 0.0002$ , 95% CI [15.60, 33.34]), performed worse on the retention trial (patients:  $6.33 \pm 1.41$ , controls:  $13.60 \pm 0.46$ ,  $Z = -3.08$ ,  $p = 0.0021$ ), as well as in delayed recall (patients:  $5.87 \pm 1.46$ , controls:  $14.07 \pm 0.36$ ,  $t(14) = 5.41$ ,  $p < 0.0001$ , 95% CI [4.95, 11.45]). Also, patients were impaired in recognizing the previously learned words compared to the healthy controls (patients:  $10.00 \pm 1.13$ , controls:  $14.60 \pm 0.16$ ,  $t(14) = 4.24$ ,  $p = 0.0002$ , 95% CI [2.27, 6.93]). Summarizing the results of the neuropsychological assessment, patients were also impaired in visuo-spatial and working memory, executive functions, as well as verbal fluency (Table 1). We did not find any correlation between the PatSep score and neuropsychological test variables in the patient group (all  $p$ 's  $> 0.142$ ), whereas the control group showed significant correlations between the PatSep

score and the learning trials of the RAVLT ( $r = 0.636$ ,  $p = 0.043$ ), visuospatial memory (all  $p$ 's  $< 0.05$ ), and working memory ( $r = 0.625$ ,  $p = 0.017$ ).

### Hippocampal volumetry

A whole-brain analysis of normalized cortical gray matter volume showed no significant reduction in patients compared to controls ( $t(14) = -1.83$ ,  $p = 0.088$ , 95% CI [-6.62, 0.52], patients:  $39.71 \pm 1.88$ , controls:  $42.76 \pm 1.40$ ). Cortical gray matter volume was not correlated to behavioral measurements of the MST neither in the patient nor in the control group (all  $p$ 's  $> 0.427$ ). With regard to the whole bilateral hippocampal volume, we found a significant reduction for patients (Table 2). A three-way repeated measures ANOVA (group  $\times$  side  $\times$  subfield) revealed significant main effects of group ( $F(1, 14) = 14.82$ ,  $p < 0.01$ ) and subfield ( $F(2, 18.06) = 1123.61$ ,  $p < 0.0001$ ), but no effect of side ( $F(1, 14) = 0.85$ ,  $p = 0.373$ ). Among two-way interactions only the group  $\times$  subfield interaction

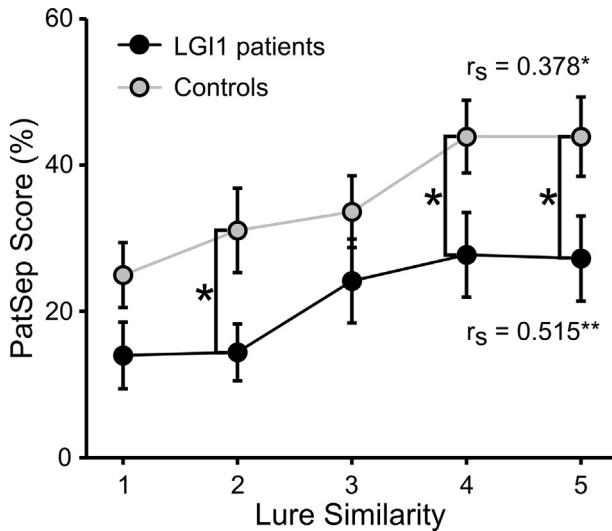


**Fig. 3.** Pattern separation performance as a function of lure similarity from 1 (most similar) to 5 (least similar). There is a significant gradual increase in pattern separation performance from high to low similarity for both the patient and control group. However, controls show superior performance in pattern separation compared to LGI1 patients from highly similar lures to lures with low similarity to targets.  $p < 0.05$ , \*\* $p < 0.01$ .

was significant ( $F(2, 28) = 10.11$ ,  $p < 0.001$ ). The three-way interaction between the included factors remained also non-significant ( $F(2, 15.67) = 0.469$ ,  $p = 0.525$ ). As we found no effects for the hippocampal sides, further analyses were based on collapsed left and right hippocampal volumes. Post-hoc pairwise comparisons showed that all analyzed subfields were significantly reduced in LGI1 patients (Table 2).

*Pattern separation performance depends on DG atrophy, whereas CA1 volume predicts recognition memory.* The volumes of CA1, CA2/3, and DG were inserted into a stepwise multiple regression model to predict pattern separation performance. The backward stepwise regression demonstrated that only the volume of the DG was a significant predictor ( $t(29) = 2.30$ ,  $p = 0.029$ , 95% CI [0.01, 0.17]) (Fig. 4A) in the statistically significant model ( $F(1, 29) = 5.30$ ,  $p = 0.029$ ) that accounted for approximately 16% of the variance of pattern separation performance. With regard to the RM score only the volume of CA1 earned entry to the

prediction model ( $t(29) = 4.75$ ,  $p < 0.001$ , 95% CI [0.001, 0.002]) (Fig. 4B). The resulting equation by removing insignificant CA2/3 and DG volume was able to explain nearly 45% of the variance of the RM score ( $F(1, 29) = 22.54$ ,  $p < 0.001$ ). All models with corresponding parameters from the backward stepwise regression analyses are presented in Table 3.

### Clinical imaging

Follow-up routine MRI data were available for 14 patients and showed hippocampal atrophy in 13 patients (92.85%). In 9 of 14 patients (64.29%), hippocampal atrophy was accompanied by T2/ FLAIR signal increase and loss of internal laminar architecture indicating hippocampal sclerosis in the dentate gyrus region (Fig. 5).

## DISCUSSION

Our study demonstrates that patients with a LGI1 encephalitis compared to healthy controls show an impaired pattern separation and recognition memory performance in combination with a global hippocampal volume loss. However, despite the global volume reduction, we found a significant structure–function relationship for pattern separation performance for the DG. Compared to the areas CA2/3 and CA1, the DG proved to be the best predictor of pattern separation performance measured by a mnemonic similarity task. Our results thus corroborate the emerging findings of human studies that pattern separation performance is especially mediated by the hippocampal DG (Bakker et al., 2008; Lacy et al., 2011). Moreover, CA1 volume predicted recognition memory performance more than any other region of interest. These findings suggest a regional specialization of hippocampal functions involved in cognitive processing.

Using the MST in combination with magnetic resonance imaging, previous fMRI studies suggested the CA3 and DG regions to be associated with pattern separation performance (Bakker et al., 2008; Lacy et al., 2011). However, in these studies CA3/DG was collapsed and studied in a unitary way due to a limitation in the resolution of imaging. Of particular importance, a recent ultra-high resolution fMRI study with 7 Tesla showed that only the DG compared to other hippocampal subfields showed separation-like activity evoked by items presented by a mnemonic similarity task, supporting our find-

**Table 1.** Neuropsychological data of LGI1 patients and controls (mean  $\pm$  SEM)

	LGI1 patients	Controls	95% CI	<i>t</i>	<i>Z</i>	<i>p</i>
RCF copy	31.80 $\pm$ 1.20	29.40 $\pm$ 1.42	[−5.67, 0.87]	−1.57	–	0.138
RCF recall	15.78 $\pm$ 2.50	28.67 $\pm$ 1.38	[7.70, 18.10]	5.32	–	0.0001
TMT-A	57.13 $\pm$ 8.28	35.87 $\pm$ 4.22	[−33, −4]	–	−2.81	0.005
TMT-B	201.13 $\pm$ 47.94	95.23 $\pm$ 14.69	[−150, −14]	–	−2.67	0.008
MWT-B*	24.29 $\pm$ 2.50	29.53 $\pm$ 1.57	[−0.29, 10.29]	2.04	–	0.062
RWT-forenames	20.47 $\pm$ 1.98	30.60 $\pm$ 1.91	[3.61, 16.66]	3.33	–	0.005
RWT-S	12.40 $\pm$ 1.61	18.20 $\pm$ 1.32	[1.00, 10.60]	2.59	–	0.021
Digit span total	11.80 $\pm$ 1.21	16.47 $\pm$ 1.03	[1.81, 7.53]	3.50	–	0.004

$t(df = 14)$ , \* $t(df = 13)$ ; RCF, Rey–Osterrieth complex figure; TMT, Trail-making test; MWT, Mehrfachwahl–Wortschatz–Intelligenztest; RWT, Regensburg word fluency test.

**Table 2.** Hippocampal volumetry (mm<sup>3</sup>) for each subfield for LGI1 patients (*n* = 15) and controls (*n* = 15)

	LGI1 patients	Controls	95% CI	<i>t</i>	<i>p</i>
CA1	544.88 ± 21.19	640.76 ± 18.06	[42.65, 149.12]	3.86	0.0029
CA2/3	182.14 ± 8.10	218.49 ± 6.15	[14.76, 57.93]	3.61	0.0029
DG	467.22 ± 19.74	554.44 ± 15.66	[36.00, 138.44]	3.65	0.003
Total hippocampal volume	2883.29 ± 112.32	3381.08 ± 95.82	[252.47, 743.09]	4.35	0.002

Volumes are presented as mean ± SEM (mm<sup>3</sup>) averaged across sides and normalized for estimated total intracranial volume. *t*(*df* = 14). Adjustment for multiple testing was done using Benjamini & Hochberg's False Discovery Rate.

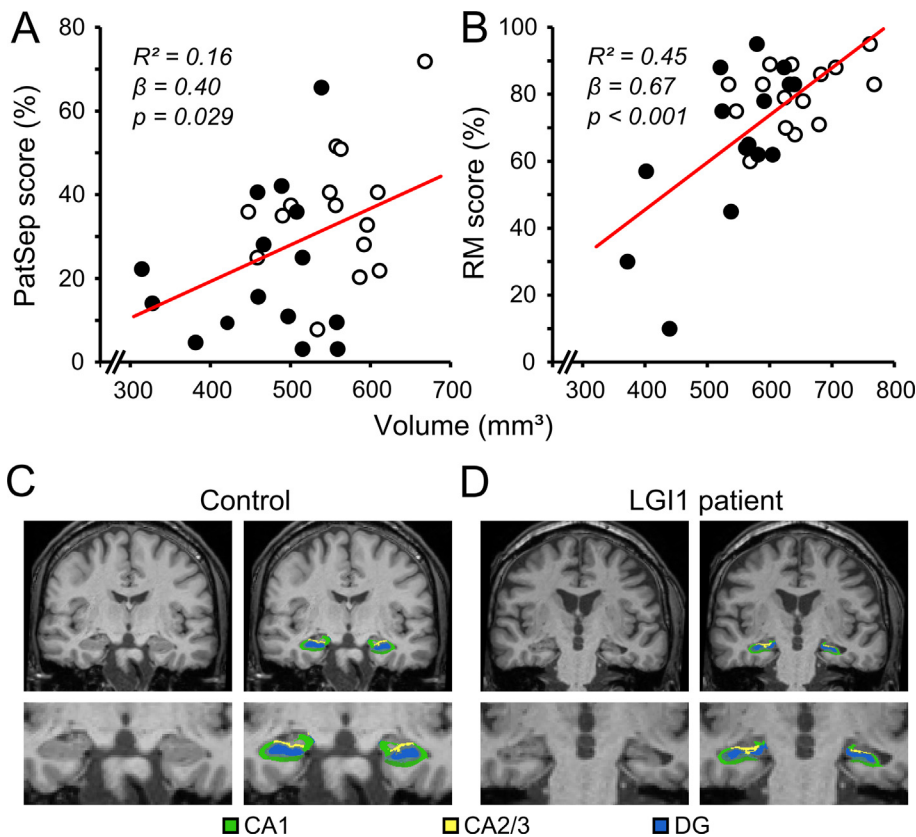


**Fig. 4.** (A)–(B) Regression lines depict the predictive model of bilateral hippocampal subfield volumes (mm<sup>3</sup>) of the DG on pattern separation and CA1 on recognition memory. Higher volumes of the DG predict higher pattern separation performance across controls (white) and LGI1 patients (black), whereas higher volumes of CA1 predict higher recognition memory performance. (C)–(D) T1-weighted MR scans of representative subjects of both the control and patient group shows the hippocampal subfield segmentation. Note the higher hippocampal volume for the control participant. PatSep, pattern separation; RM, recognition memory CA, cornu ammonis; DG, dentate gyrus.

ing of a preferential involvement of the DG in pattern separation performance in humans (Berron et al., 2016). In addition, a recent case study examining a patient with bilateral ischemic lesions in the DG further suggested a particular role for the DG in pattern separation as the impaired patient performed slightly worse on the MST compared to a healthy control group (Baker et al., 2016).

Data from recent human studies demonstrated deficits in behavioral pattern separation in patients with amnesic mild cognitive impairment (Yassa et al., 2010; Stark et al., 2013), Alzheimer's disease (Ally et al., 2013), and traumatic brain injury (Kirwan et al., 2012). Similarly, healthy aged humans showed deficits in pattern separation through a decline of pattern separation ability during aging (Toner et al., 2009; Stark et al., 2010; Yassa et al., 2011a; Holden et al., 2013; Stark et al., 2013, 2015). The present data thus complement the current view on pattern separation dependent on hippocampal integrity in the context of disease-related structural as well as age-related changes in humans. Moreover, we additionally studied mnemonic

**Table 3.** Stepwise linear regression model to predict the PatSep and RM scores from variability in hippocampal subfield volume

PatSep	Model 1			Model 2			Model 3			
	Variable	B	SE (B)	β	B	SE (B)	β	B	SE (B)	β
CA1		−0.040	0.107	−0.201						
CA2/3		−0.401	0.330	−0.747	−0.394	0.324	−0.733			
DG		0.286	0.180	1.306	0.241	0.132	1.102	0.088	0.038	0.399*
R <sup>2</sup>			0.207			0.203			0.159	
RM										
Variable	B	SE (B)	β	B	SE (B)	β	B	SE (B)	β	
CA1	0.002	0.001	0.783	0.002	0.001	0.762*	0.001	0.0003	0.668***	
CA2/3	−0.0004	0.003	−0.076	−0.001	0.002	−0.104				
DG	−0.0001	0.002	−0.050							
R <sup>2</sup>			0.448			0.448			0.446	

B, unstandardized coefficient; SE (B) standard error of the coefficient; β, beta coefficient, \**p* < 0.05, \*\*\**p* < 0.001.

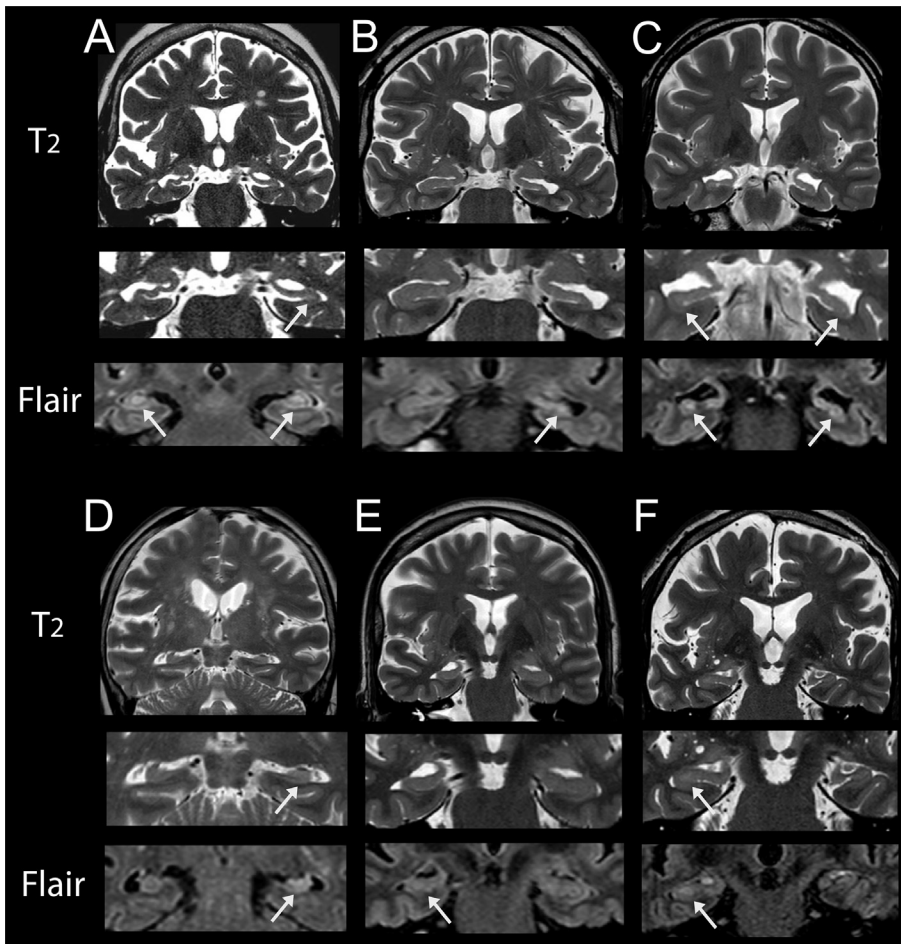


**Fig. 5.** A–F: Representative clinical MR images of six patients with LGI1 encephalitis during follow-up and time point of testing. Top row: Coronal T2-weighted imaging showing bilateral (A, C, D) or unilateral (B, E, F) hippocampal atrophy. Magnification shows atrophy of all hippocampal cortical layers including CA1 and a predominant atrophy of the dentate gyrus region including loss of internal laminar architecture in CA4/DG. Coronal FLAIR imaging shows signal hyperintensities in hippocampal region CA4/DG (arrows).

processing of stimuli with high or low similarity to a corresponding target. Our patient cohort showed impairments in pattern separation graded across all similarity levels, a finding that is reminiscent of the behavioral outcome found in healthy aging (Yassa et al., 2011a; Stark et al., 2013). Indeed, a preferential degradation of DG function has been implicated in aging processes (West, 1993; Small et al., 2002; Yassa et al., 2011b).

On a neural level, computational models suggest that within the hippocampal network, the DG performs pattern separation by a decorrelation of overlapping neural assemblies at encoding (Treves and Rolls, 1994; Rolls, 2016). This concept is supported by a variety of experimental rodent studies showing that the hippocampal DG is indeed involved in pattern separation, whereas the area CA3 performs pattern completion (Leutgeb et al., 2007; Leutgeb and Leutgeb, 2007; McHugh et al., 2007; Neunuebel and Knierim, 2014). In the process of pattern completion within CA3, the interconnection of pyramidal neurons functions as an auto-associative network so that a stored representation can be retrieved from an incoming

partial cue (O'Reilly and McClelland, 1994; Norman and O'Reilly, 2003). Considering this, it has been suggested that the interplay of the DG and CA3 within the tri-synaptic circuit of the hippocampus is a reflection of a putative concomitant functional interdependence of pattern separation and completion as a result of a dynamic process-inherent trade-off depending on the current state of input-dependent system requirements (O'Reilly and McClelland, 1994; Lisman, 1999). In this process, CA3 is assumed to be able to switch between pattern separation and completion based on input similarity (Vazdarjanova and Guzowski, 2004; Leutgeb et al., 2007; Knierim and Neunuebel, 2016). In this connection, we showed in another study that the process of pattern separation in the hippocampus is strongly influenced by oscillatory dynamics during sleep so that memory representations are stabilized (Hanert et al., 2017). Judging from the inherent network anatomy of the DG-CA3 networks in our patients, it seems plausible that a dysfunctional DG with its strong projections onto CA3 also affects the downstream network functions of CA3 itself. Here, we assume that the hippocampal circuit disruption in our patient cohort caused the deficits in pattern separation compared to our healthy control group. However, regarding the DG-CA3 network embedded in the tri-synaptic circuit, the DG volume turned out to be a better predictor of pattern separation performance compared to CA2/3. Considering the dysfunctional and lesioned DG-CA3 network in our patients the CA2/3 region failed to reach significance in the model probably due to the strong dependency of CA3's pattern separation function on intact DG inputs.

Of note, we could not show a significant prediction of pattern separation performance by CA1. However, recent imaging findings in humans showed that CA1 exhibits pattern separation-like activity when the input similarity is low (i.e., when the change of the input increases) (Lacy et al., 2011). Recordings from CA1 and CA3 cells in rodents likewise suggest a linear transfer function of CA1, whereas CA3 responds in a non-linear fashion (i.e., with pattern separation like activity for both small and large environmental changes) (Guzowski et al., 2004; Leutgeb et al., 2005). In that sense, both human and rodent studies showed that CA1 is able to exhibit pat-

tern separation, provided that the change of the input was large (Lee et al., 2004; Leutgeb et al., 2005; Lacy et al., 2011). However, as we presented both large and small input changes, it is possible that the effect of CA1 variability on pattern separation was dampened. Overall, given the sequential processing of mnemonic information in the DG, CA3 and CA1 network in the hippocampal trisynaptic circuit, we show despite the global atrophic changes in hippocampal regions the highest prediction of pattern separation performance by the DG structure supporting the special role of the DG in pattern separation processes in humans.

In addition to impaired pattern separation, our patients showed decreased recognition memory. These results are in accordance with previous studies using mnemonic similarity tasks to consider hippocampal efficiency in memory impaired patients (Yassa et al., 2010; Ally et al., 2013). Given the fact that poor memory recovery due to hippocampal atrophy is common in patients with LGI1 encephalitis (Malter et al., 2014) this finding was actually not surprising. The persisting cognitive deficits are most likely a reflection of the severity of the encephalitis on hippocampal functions in our patients as also seen in the hippocampal atrophy. More importantly, in our study cohort, the volume of the hippocampal area CA1 was the best predictor of recognition memory performance. CA1 as the output relay area of the hippocampus receives input from CA3 via the Schaffer collaterals that converges with entorhinal input via the perforant path (Insausti and Amaral, 2004; van Strien et al., 2009). It is assumed that CA1 compares the converging mnemonic representations from hippocampal CA3 and information about the actual present state carried by entorhinal input pattern (Vinogradova, 2001; Hasselmo, 2005; Knierim and Neunuebel, 2016). This ideal location of CA1 facilitates a full retrieval of memory traces and information that fully matches the actual state (Hasselmo and Wyble, 1997; Hasselmo and Eichenbaum, 2005). Accordingly, previous studies ascribed the function of novelty detection in the sense of a match/mismatch computation in memory processing to CA1 (Lisman, 1999; Duncan et al., 2012; Reagh et al., 2014; Knierim and Neunuebel, 2016). Thus, the position of CA1 that enables to retrieve a complete memory pattern due to an integration of mnemonic inputs from different subnetworks clearly explains the highly predictive value of the CA1 volume regarding recognition memory performance in our study. Notably, neither recognition memory nor any other neurocognitive domain were correlated with pattern separation performance in LGI1 patients arguing against the possibility that the pattern separation impairment was secondary to cognitive deficits. Our results reflect a functional dissociation of pattern separation and recognition memory performance which might suggest that both computations are relayed by different hippocampal subnetworks. However, future experimental models have to further differentiate network-related mechanisms that affect distinct cognitive and behavioral outcome in humans.

Interestingly, Miller et al. (2017) showed a significant LGI1 encephalitis-induced hippocampal volume loss

restricted to bilateral CA3, in contrast to the global volume reduction that was apparent in our data. The difference might be due to the segmentation method used to analyze ultra-high field 7T MR images. However, it might be mentioned that, the examined LGI1 patients in the Miller study also showed a global hippocampal volume reduction, although not reaching significance levels. Hence, it is more likely that the global volume reduction that we observed may be better explained by a stronger noxious impact on the hippocampus due to stronger hippocampal inflammation in the acute phase leading to a greater disease severity of our study cohort. Indeed, we have shown a particular vulnerability of the hippocampus in encephalitis (Bartsch et al., 2015). Also, it is plausible that the epilepsy in the acute phase with subsequent hippocampal sclerosis in the DG further contributed to the structural sequelae in our cohort (Blümcke et al., 2013b, 2013a; Coras et al., 2014). It is, hence, important to note that pattern separation and completion deficits in the hippocampus may not exclusively be determined by atrophic changes but that memory processing deficits may also be the result of dysfunctional cellular and neuroplastic network alterations in the course of the disease process without leading to neurodegeneration and atrophy. In this vein, Coras et al. (2014) showed that cognitive deficits in patients with epilepsy due to hippocampal dysfunction and hippocampal sclerosis was not associated with atrophy but with cellular changes in hippocampal subfields. Thus, the dysfunction of memory processing can also be caused by subregional network dysfunction that may not lead in atrophic sequelae in the hippocampus.

In addition, the examination of damaged brain tissue can influence automated segmentation sensitivity. In patients with hippocampal sclerosis, automated segmentation by means of Freesurfer showed a greater difference to manual segmentation compared to the healthy brain (Pardoe et al., 2009). In this sense, our results may be confounded by a higher segmentation error in the patient group. However, supporting the reliability of our findings, it has been shown that Freesurfer's segmentation algorithm was sensitive to hippocampal atrophy in patients with mesial temporal lobe epilepsy; and, importantly, those results correlated with those of a manual segmentation technique (Morey et al., 2009; Pardoe et al., 2009). We have acknowledged the issue of a variability in segmentation due to an underlying pathology by visual inspection of the clinical MRI scans (Fig. 5) that indicate the particular affection of the DG region thus corroborating the main effect of the DG lesioning on hippocampal functions.

It has to be considered that a deficit in pattern separation – as shown in our study cohort by diminished correct 'similar' response to lures – should be also reflected by a heightened false 'old' response to lures (i.e. a shift toward pattern completion) (Yassa et al., 2010; Ally et al., 2013). However, our patient cohort showed an equal proportion of 'old' answers to lures compared with the healthy control group probably indicating that pattern completion processes were not affected by the present hippocampal atrophy. However, as a caveat and limiting the interpretation of pattern completion perfor-

mance, the MST lacks specificity regarding partial cues that reactivate previously encoded mnemonic representations (Hunsaker and Kesner, 2013). We thus based our analysis and conclusions of behavioral data on pattern separation. Indeed, the assessment of pattern separation performance based on the MST has been shown in a variety of studies (Lacy et al., 2011; Stark et al., 2013; Yassa et al., 2010; Yassa et al., 2011b).

In conclusion, our findings show that patients with LGI1 limbic encephalitis were impaired in pattern separation and recognition memory performance that can be traced back to hippocampal volume reduction and loss of hippocampal integrity. The facts that the LGI1 gene transcript is mainly expressed in DG and CA3 neurons (Kalachikov et al., 2002; Herranz-Pérez et al., 2010) and a deficiency of LGI1 selectively decreases synaptic transmission in the hippocampus (Fukata et al., 2010), emphasize the basic principle of the structure–function relationship between hippocampal subfields and memory processing. Specifically, the variability of the DG was predictive of behavioral pattern separation performance compatible with the current view on the DG to be involved in hippocampal pattern separation. By contrast, recognition memory was strongest predicted by the volume of CA1. These findings show that LGI1 encephalitis differentially targets distinct subregions of the hippocampal circuit and corroborate the framework of a regional specialization of hippocampal functions involved in cognitive processing.

## ACKNOWLEDGMENTS

The present study was supported by Deutsche Forschungsgemeinschaft (SFB 654, A14, “Plasticity and Sleep” and FOR 2093) and the Medical Faculty of the University of Kiel. The authors declare no competing financial interests. T.B. and A.H. designed the experiments, A.H., T.B. and J.R. carried out the experiments, A.H., T.B., and J.B. analyzed the data and A.H., J.R., O.G., M.Z., A.P., J.B., C.F., and T.B. wrote the paper.

## REFERENCES

- Ally BA, Hussey EP, Ko PC, Molitor RJ (2013) Pattern separation and pattern completion in Alzheimer's disease: evidence of rapid forgetting in amnesic mild cognitive impairment. *Hippocampus* 23:1246–1258.
- Amaral DG, Scharfman HE, Lavenex P (2007) The dentate gyrus: fundamental neuroanatomical organization (dentate gyrus for dummies). *Prog Brain Res* 163:3–22.
- Aschenbrenner S, Tucha O, Lange KW (2000) Regensburger Wortflüssigkeitstest. Göttingen: Testzentrale.
- Baker S, Vieweg P, Gao F, Gilboa A, Wolbers T, Black SE, Rosenbaum RS (2016) The human dentate gyrus plays a necessary role in discriminating new memories. *Curr Biol* 26:2629–2634.
- Bakker A, Kirwan CB, Miller M, Stark CEL (2008) Pattern separation in the human hippocampal CA3 and dentate gyrus. *Science* 319:1640–1642.
- Bartsch T, Döhring J, Reuter S, Finke C, Rohr A, Brauer H, Deuschl G, Jansen O (2015) Selective neuronal vulnerability of human hippocampal CA1 neurons: lesion evolution, temporal course, and pattern of hippocampal damage in diffusion-weighted MR imaging. *J Cereb Blood Flow Metab* 35:1836–1845.
- Bartsch T, Döhring J, Rohr A, Jansen O, Deuschl G (2011) CA1 neurons in the human hippocampus are critical for autobiographical memory, mental time travel, and autoethic consciousness. *Proc Natl Acad Sci U S A* 108:17562–17567.
- Bartsch T, Schönfeld R, Müller FJ, Alfke K, Lepow B, Aldenhoff J, Deuschl G, Koch JM (2010) Focal lesions of human hippocampal CA1 neurons in transient global amnesia impair place memory. *Science* 328:1412–1415.
- Bartsch T, Wulff P (2015) The hippocampus in aging and disease: from plasticity to vulnerability. *Neuroscience* 309:1–16.
- Berron D, Schütze H, Maass A, Cardenas-Blanco A, Kuijf HJ, Kumaran D, Düzel E (2016) Strong evidence for pattern separation in human dentate gyrus. *J Neurosci* 36:7569–7579.
- Bettcher BM, Gelfand JM, Irani SR, Neuhaus J, Forner S, Hess CP, Geschwind MD (2014) More than memory impairment in voltage-gated potassium channel complex encephalopathy. *Eur J Neurol* 21:1301–1310.
- Blümcke I, Thom M, Aronica E, Armstrong DD, Bartolomei F, Bernasconi A, Bernasconi N, Bien CG, et al. (2013a) International consensus classification of hippocampal sclerosis in temporal lobe epilepsy: a Task Force report from the ILAE Commission on Diagnostic Methods. *Epilepsia* 54:1315–1329.
- Blümcke I, Cross JH, Spreafico R (2013b) The international consensus classification for hippocampal sclerosis: an important step towards accurate prognosis. *Lancet Neurol* 12:844–846.
- Buckner RL, Head D, Parker J, Fotenos AF, Marcus D, Morris JC, Snyder AZ (2004) A unified approach for morphometric and functional data analysis in young, old, and demented adults using automated atlas-based head size normalization: reliability and validation against manual measurement of total intracranial volume. *NeuroImage* 23:724–738.
- Butler CR, Miller TD, Kaur MS, Baker IW, Boothroyd GD, Illman NA, Rosenthal CR, Vincent A, et al. (2014) Persistent anterograde amnesia following limbic encephalitis associated with antibodies to the voltage-gated potassium channel complex. *J Neurol Neurosurg Psychiatry* 85:387–391.
- Coras R, Pauli E, Li J, Schwarz M, Rössler K, Buchfelder M, Hamer H, Stefan H, et al. (2014) Differential influence of hippocampal subfields to memory formation – insights from TLE patients. *Brain* 137:1945–1957.
- Döhring J, Stoldt A, Witt K, Schönfeld R, Deuschl G, Born J, Bartsch T (2017) Motor skill learning and offline-changes in TGA patients with acute hippocampal CA1 lesions. *Cortex* 89:156–168.
- Duncan K, Ketz N, Inati SJ, Davachi L (2012) Evidence for area CA1 as a match/mismatch detector: a high-resolution fMRI study of the human hippocampus. *Hippocampus* 22:389–398.
- Finke C, Prüss H, Heine J, Reuter S, Kopp UA, Wegner F, Then Bergh F, Koch S, et al. (2017) Evaluation of cognitive deficits and structural hippocampal damage in encephalitis with leucine-rich, glioma-inactivated 1 antibodies. *JAMA Neurol* 74:50–59.
- Fischl B, Salat DH, van der Kouwe AJW, Makris N, Ségonne F, Quinn BT, Dale AM (2004) Sequence-independent segmentation of magnetic resonance images. *NeuroImage* 23:S69–S84.
- Fukata Y, Lovero KL, Iwanaga T, Watanabe A, Yokoi N, Tabuchi K, Shigemoto R, Nicoll RA, et al. (2010) Disruption of LGI1-linked synaptic complex causes abnormal synaptic transmission and epilepsy. *Proc Natl Acad Sci U S A* 107:3799–3804.
- Guzowski JF, Knierim JJ, Moser EI (2004) Ensemble dynamics of hippocampal regions CA3 and CA1. *Neuron* 44:581–584.
- Hanert A, Weber FD, Pedersen A, Born J, Bartsch T (2017) Sleep in humans stabilizes pattern separation performance. *J Neurosci* 37:12238–12246.
- Hasselmo ME (2005) The role of hippocampal regions CA3 and CA1 in matching entorhinal input with retrieval of associations between objects and context: theoretical comment on Lee et al. (2005). *Behav Neurosci* 119:342–345.
- Hasselmo ME, Eichenbaum H (2005) Hippocampal mechanisms for the context-dependent retrieval of episodes. *Neural Netw* 18:1172–1190.

- Hasselmo ME, Wyble BP (1997) Free recall and recognition in a network model of the hippocampus: simulating effects of scopolamine on human memory function. *Behav Brain Res* 89:1–34.
- Herranz-Pérez V, Olucha-Bordonau FE, Morante-Redolat JM, Pérez-Tur J (2010) Regional distribution of the leucine-rich glioma inactivated (LGI) gene family transcripts in the adult mouse brain. *Brain Res* 1307:177–194.
- Holden HM, Toner C, Pirogovsky E, Kirwan CB, Gilbert PE (2013) Visual object pattern separation varies in older adults. *Learn Mem* 20:358–362.
- Hunsaker MR, Kesner RP (2013) The operation of pattern separation and pattern completion processes associated with different attributes or domains of memory. *Neurosci Biobehav Rev* 37:36–58.
- Iglesias JE, Augustinack JC, Nguyen K, Player CM, Player A, Wright M, Roy N, Frosch MP, et al. (2015) A computational atlas of the hippocampal formation using ex vivo, ultra-high resolution MRI: application to adaptive segmentation of in vivo MRI. *NeuroImage* 115:117–137.
- Insausti R, Amaral DG (2004) Hippocampal formation. In: Paxinos G, editor. *The human nervous system*. Amsterdam: Elsevier. p. 871–914.
- Irani SR, Michell AW, Lang B, Pettingill P, Waters P, Johnson MR, Schott JM, Armstrong RJE, et al. (2011) Faciobrachial dystonic seizures precede Lgi1 antibody limbic encephalitis. *Ann Neurol* 69:892–900.
- Irani SR, Stagg CJ, Schott JM, Rosenthal CR, Schneider SA, Pettingill P, Pettingill R, Waters P, et al. (2013) Faciobrachial dystonic seizures: the influence of immunotherapy on seizure control and prevention of cognitive impairment in a broadening phenotype. *Brain* 136:3151–3162.
- Kalachikov S, Evgrafov O, Ross B, Winawer M, Barker-Cummings C, Boneschi FM, Choi C, Morozov P, et al. (2002) Mutations in LGI1 cause autosomal-dominant partial epilepsy with auditory features. *Nat Genet* 30:335–341.
- Kirwan CB, Hartshorn A, Stark SM, Goodrich-Hunsaker NJ, Hopkins RO, Stark CEL (2012) Pattern separation deficits following damage to the hippocampus. *Neuropsychologia* 50:2408–2414.
- Kirwan CB, Stark CEL (2007) Overcoming interference: an fMRI investigation of pattern separation in the medial temporal lobe. *Learn Mem* 14:625–633.
- Knierim JJ, Neunuebel JP (2016) Tracking the flow of hippocampal computation: pattern separation, pattern completion, and attractor dynamics. *Neurobiol Learn Mem* 129:38–49.
- Lacy JW, Yassa MA, Stark SM, Muftuler LT, Stark CEL (2011) Distinct pattern separation related transfer functions in human CA3/dentate and CA1 revealed using high-resolution fMRI and variable mnemonic similarity. *Learn Mem* 18:15–18.
- Lee I, Yoganasimha D, Rao G, Knierim JJ (2004) Comparison of population coherence of place cells in hippocampal subfields CA1 and CA3. *Nature* 430:456–459.
- Lehrl S (2005) *Mehrfachwahl-Wortschatz-Intelligenz-Test, MWT-B*. 5th ed. Balingen: Spitta Verlag.
- Leutgeb JK, Leutgeb S, Moser MB, Moser EI (2007) Pattern separation in the dentate gyrus and CA3 of the hippocampus. *Science* 315:961–966.
- Leutgeb JK, Leutgeb S, Treves A, Meyer R, Barnes CA, McNaughton BL, Moser MB, Moser EI (2005) Progressive transformation of hippocampal neuronal representations in “morphed” environments. *Neuron* 48:345–358.
- Leutgeb S, Leutgeb JK (2007) Pattern separation, pattern completion, and new neuronal codes within a continuous CA3 map. *Learn Mem* 14:745–757.
- Leutgeb S, Leutgeb JK, Treves A, Moser MB, Moser EI (2004) Distinct ensemble codes in hippocampal areas CA3 and CA1. *Science* 305:1295–1298.
- Lisman JE (1999) Relating hippocampal circuitry to function: recall of memory sequences by reciprocal dentate-CA3 interactions. *Neuron* 22:233–242.
- Malter MP, Frisch C, Schoene-Bake JC, Helmstaedter C, Wandinger KP, Stoecker W, Urbach H, Surges R, et al. (2014) Outcome of limbic encephalitis with VGKC-complex antibodies: relation to antigenic specificity. *J Neurol* 261:1695–1705.
- McClelland JL, McNaughton BL, O'Reilly RC (1995) Why there are complementary learning systems in the hippocampus and neocortex: insights from the successes and failures of connectionist models of learning and memory. *Psychol Rev* 102:419–457.
- McHugh TJ, Jones MW, Quinn JJ, Balthasar N, Coppari R, Elmquist JK, Lowell BB, Fanselow MS, et al. (2007) Dentate gyrus NMDA receptors mediate rapid pattern separation in the hippocampal network. *Science* 317:94–99.
- Miller TD, Chong TT-J, Aimola Davies AM, Ng TWC, Johnson MR, Irani SR, Vincent A, Husain M, et al. (2017) Focal CA3 hippocampal subfield atrophy following LGI1 VGKC-complex antibody limbic encephalitis. *Brain* 140:1212–1219.
- Morey R-A, Petty CM, Xu Y, Pannu Hayes J, Wagner HR, Lewis DV, LaBar KS, Styner M, et al. (2009) A comparison of automated segmentation and manual tracing for quantifying hippocampal and amygdala volumes. *NeuroImage* 45:855–866.
- Neunuebel JP, Knierim JJ (2014) CA3 retrieves coherent representations from degraded input: direct evidence for CA3 pattern completion and dentate gyrus pattern separation. *Neuron* 81:416–427.
- Norman KA, O'Reilly RC (2003) Modeling hippocampal and neocortical contributions to recognition memory: a complementary-learning-systems approach. *Psychol Rev* 110:611–646.
- O'Reilly RC, McClelland JL (1994) Hippocampal conjunctive encoding, storage, and recall: avoiding a trade-off. *Hippocampus* 4:661–682.
- Pardoe HR, Pell GS, Abbott DF, Jackson GD (2009) Hippocampal volume assessment in temporal lobe epilepsy: how good is automated segmentation? *Epilepsia* 50:2586–2592.
- Reagh ZM, Watabe J, Ly M, Murray E, Yassa MA (2014) Dissociated signals in human dentate gyrus and CA3 predict different facets of recognition memory. *J Neurosci* 34:13301–13313.
- Reitan RM (1979) *Trail Making Test (TMT)*. Göttingen: Hogrefe.
- Rey A (1941) L'examen psychologique dans les cas d'encéphalopathie traumatique. *Arch Psychol* 28:21.
- Rolls ET (2016) Pattern separation, completion, and categorisation in the hippocampus and neocortex. *Neurobiol Learn Mem* 129:4–28.
- Ségonne F, Dale AM, Busa E, Glessner M, Salat D, Hahn HK, Fischl B (2004) A hybrid approach to the skull stripping problem in MRI. *NeuroImage* 22:1060–1075.
- Ségonne F, Pacheco J, Fischl B (2007) Geometrically accurate topology-correction of cortical surfaces using nonseparating loops. *IEEE Trans Med Imaging* 26:518–529.
- Sled JG, Zijdenbos AP, Evans AC (1998) A nonparametric method for automatic correction of intensity nonuniformity in MRI data. *IEEE Trans Med Imaging* 17:87–97.
- Small SA, Tsai WY, DeLaPaz R, Mayeux R, Stern Y (2002) Imaging hippocampal function across the human life span: is memory decline normal or not? *Ann Neurol* 51:290–295.
- Stark SM, Stevenson R, Wu C, Rutledge S, Stark CEL (2015) Stability of age-related deficits in the mnemonic similarity task across task variations. *Behav Neurosci* 129:257–268.
- Stark SM, Yassa MA, Lacy JW, Stark CEL (2013) A task to assess behavioral pattern separation (BPS) in humans: data from healthy aging and mild cognitive impairment. *Neuropsychologia* 51:2442–2449.
- Stark SM, Yassa MA, Stark CEL (2010) Individual differences in spatial pattern separation performance associated with healthy aging in humans. *Learn Mem* 17:284–288.
- Toner CK, Pirogovsky E, Kirwan CB, Gilbert PE (2009) Visual object pattern separation deficits in nondemented older adults. *Learn Mem* 16:338–342.
- Treves A, Rolls ET (1994) Computational analysis of the role of the hippocampus in memory. *Hippocampus* 4:374–391.

- Van Leemput K, Bakkour A, Benner T, Wiggins G, Wald LL, Augustinack J, Dickerson BC, Golland P, et al. (2009) Automated segmentation of hippocampal subfields from ultra-high resolution in vivo MRI. *Hippocampus* 19:549–557.
- van Strien NM, Cappaert NL, Witter MP (2009) The anatomy of memory: an interactive overview of the parahippocampal-hippocampal network. *Nat Rev Neurosci* 10:272–282.
- Vazdarjanova A, Guzowski JF (2004) Differences in hippocampal neuronal population responses to modifications of an environmental context: evidence for distinct, yet complementary, functions of CA3 and CA1 ensembles. *J Neurosci* 24:6489–6496.
- Vinogradova OS (2001) Hippocampus as comparator: role of the two input and two output systems of the hippocampus in selection and registration of information. *Hippocampus* 11:578–598.
- West MJ (1993) Regionally specific loss of neurons in the aging human hippocampus. *Neurobiol Aging* 14:287–293.
- Yassa MA, Lacy JW, Stark SM, Albert MS, Gallagher M, Stark CEL (2011a) Pattern separation deficits associated with increased hippocampal CA3 and dentate gyrus activity in nondemented older adults. *Hippocampus* 21:968–979.
- Yassa MA, Mattfeld AT, Stark SM, Stark CEL (2011b) Age-related memory deficits linked to circuit-specific disruptions in the hippocampus. *Proc Natl Acad Sci U S A* 108:8873–8878.
- Yassa MA, Stark CEL (2011) Pattern separation in the hippocampus. *Trends Neurosci* 34:515–525.
- Yassa MA, Stark SM, Bakker A, Albert MS, Gallagher M, Stark CEL (2010) High-resolution structural and functional MRI of hippocampal CA3 and dentate gyrus in patients with amnesic Mild Cognitive Impairment. *NeuroImage* 51:1242–1252.

*(Received 3 October 2018, Accepted 25 December 2018)*  
*(Available online 6 January 2019)*